

See discussions, stats, and author profiles for this publication at: <https://www.researchgate.net/publication/224908460>

Combined X-ray Diffraction and Density Functional Study of $[\text{Ni}(\text{NO})(\eta^5\text{-Cp}^*)]$ in the Ground and Light-Induced Metastable States

ARTICLE · JANUARY 1998

CITATIONS

18

READS

28

3 AUTHORS, INCLUDING:



Thomas R Furlani

University at Buffalo, The State University of ...

57 PUBLICATIONS 2,530 CITATIONS

SEE PROFILE



Philip Coppens

University at Buffalo, The State University of ...

470 PUBLICATIONS 15,840 CITATIONS

SEE PROFILE

Combined X-ray Diffraction and Density Functional Study of $[\text{Ni}(\text{NO})(\eta^5\text{-Cp}^*)]$ in the Ground and Light-Induced Metastable States

Dmitry V. Fomitchev, Thomas R. Furlani, and Philip Coppens*

Department of Chemistry, Natural Sciences Complex, State University of New York at Buffalo, Buffalo, New York 14260-3000

Received October 28, 1997

The crystal structure of $[\text{Ni}(\text{NO})(\eta^5\text{-Cp}^*)]$ in the light-induced metastable state was determined by X-ray diffraction at 25 K of a crystal with a 47% metastable-state population. The most significant geometrical change is the formation of a side (η^2) bound structure with an Ni–N–O angle of $92(1)^\circ$, compared with $179.2(2)^\circ$ in the most stable configuration, and a corresponding Ni–O distance of 2.09 Å. An elongation of the Ni–N bond by 0.08(1) Å and local distortions in the pentamethylcyclopentadienyl ring are also observed. Geometry optimizations, carried out using density functional theory, confirm that the $[\text{Ni}(\eta^2\text{-NO})(\eta^5\text{-Cp}^*)]$ structure corresponds to a local minimum with energy 0.99 eV above that of the stable isomer and predict a second local minimum at 1.85 eV for the isonitrosyl, $[\text{Ni}(\text{ON})(\eta^5\text{-Cp}^*)]$, structure. Geometrical parameters obtained from the theoretical calculation for $[\text{Ni}(\eta^2\text{-NO})(\eta^5\text{-Cp}^*)]$ agree reasonably well with the experimental findings. This is the first example of a side-bound nitrosyl complex generated by photoirradiation of an $\{\text{M}(\text{NO})\}^{10}$ ground-state configuration. Its geometry is comparable with that of the photoinduced metastable state (MS_2) of sodium nitroprusside, which in its ground state has the $\{\text{M}(\text{NO})\}^6$ configuration.

Introduction

The study of photoinduced changes in molecular crystals is of considerable importance for the understanding of photochemical processes. In the course of our investigation of light-induced metastable states of transition metal nitrosyls $\text{Na}_2[\text{Fe}(\text{CN})_5(\text{NO})] \cdot 2\text{H}_2\text{O}^1$ and $\text{K}_2[\text{Ru}(\text{NO}_2)_4(\text{NO})(\text{OH})]_2$, we have found that at sufficiently low temperature linkage isomers with an η^2 - or oxygen-bound NO group can be generated in the crystals of these compounds upon irradiation with light of specific wavelength. Until now, the observation of iso- or η^2 -bound NO has been limited to complexes of the iron family (Fe, Ru, and Os). According to the nomenclature introduced by Enemark and Feltham,³ in which the d electrons are counted together with those electrons occupying π^* levels on the NO ligand, all of these complexes can be described as $\{\text{M}(\text{NO})\}^6$.

In the present work we report the first experimental observation of η^2 -bound nickel nitrosyl generated in the single crystal of (pentamethylcyclopentadienyl)nitrosylnickel, $[\text{Ni}(\text{NO})(\eta^5\text{-Cp}^*)]$, by irradiation with 458 nm light at 25 K. This complex has an $\{\text{M}(\text{NO})\}^{10}$ electronic configuration in the ground state.

The photochemistry of (cyclopentadienyl)nitrosylnickel, $[\text{Ni}(\text{NO})(\eta^5\text{-Cp})]$, in inert matrixes (Ar, CH_4 , and N_2) at 20 K first was explored by Crichton and Rest.⁴ They found that irradiation of the sample with ultraviolet light ($230 < \lambda < 280$ nm) caused a 40% reduction of intensity of the band at 1839 cm^{-1} assigned to the stretching vibration of NO and produced a new intense band at 1392 cm^{-1} . They report that the effect also occurs at longer wavelengths, up to about 500 nm. Thermal and light-induced reversibility of the reaction was also evident. Formation

of an ion pair $[\text{Ni}(\eta^5\text{-Cp})]^+[\text{NO}]^-$ or an extreme case of intramolecular electron transfer to the nitrosyl ligand was considered as a possible explanation for the observed phenomena. The possibility of formation of the isonitrosyl complex $[\text{Ni}(\text{ON})(\eta^5\text{-Cp})]$ was also mentioned, but ruled out, as no satisfactory precedent existed for this type of structure. Therefore, on the basis of only the spectroscopic data (IR and UV/vis), the authors could not arrive at a definitive conclusion about the nature of the species produced.

Chen and co-workers⁵ reported the structures of $[\text{Ni}(\text{NO})(\eta^5\text{-Cp})]$ in the ground and light-induced states derived from EXAFS data. They were able to determine the population of the light-induced species as 57(3)%. Their two major conclusions, regarding the structure in the light-induced state, were (i) the elongation of the Ni–N bond by 0.12(3) Å and (ii) bending of the Ni–N–O fragment from 180 to $160\text{--}133^\circ$. The accuracy of their results was limited by several factors. As multiple backscattering is very sensitive to the bending angle, there is no ideal reference compound for bent Ni–N–O, unless the exact bending angle is known. Another source for the uncertainty was the fact that the N–O distance had to be fixed and kept constant throughout the calculations. On the basis of the observation that the forward and reverse reactions could be induced by light with an energy difference of 2400 cm^{-1} (280 nm for the forward reaction vs 300 nm for the reverse reaction), which is too small to separate any two electronic states, the authors suggested that at least one other state was involved in the reaction and that the bent NiNO geometry results from the relaxation of an initially excited state.

To investigate if the photochemistry of $\{\text{M}(\text{NO})\}^{10}$ complexes is related to that of complexes with an $\{\text{M}(\text{NO})\}^6$ configuration, we selected $[\text{Ni}(\text{NO})(\eta^5\text{-Cp}^*)]$ as a candidate for a structural

(1) Carducci, M. D.; Pressprich, M. R.; Coppens, P. *J. Am. Chem. Soc.* **1997**, *119*, 2669.

(2) Fomitchev, D. V.; Coppens, P. *Inorg. Chem.* **1996**, *35*, 702.

(3) Enemark, J. H.; Feltham, R. D. *Coord. Chem. Rev.* **1974**, *13*, 339.

(4) Crichton, O.; Rest, A. J. *J. Chem. Soc., Dalton Trans.* **1977**, 986.

(5) Chen, X. L.; Bowman, M. K.; Wang, Z.; Montano, P. A.; Norris, J. R. *J. Phys. Chem.* **1994**, *98*, 9457.

study combining low-temperature X-ray crystallography and photochemistry, using a new technique developed in our group several years ago.⁶

Experimental Section

Sample Preparation. We selected $[\text{Ni}(\text{NO})(\eta^5\text{-Cp}^*)]$, as it is a solid at room temperature, unlike $[\text{Ni}(\text{NO})(\eta^5\text{-Cp})]$, which is a liquid, thus avoiding experimental complications. The complex was prepared by a procedure similar to that described for $[\text{Ni}(\text{NO})(\eta^5\text{-Cp})]$.⁷ A solution of 1 g of bis(pentamethylcyclopentadienyl)nickel, $[\text{Ni}(\eta^5\text{-Cp}^*)_2]$ (Strem Chemicals Inc.), in 60 mL of pentane was treated with nitric oxide (Aldrich) at atmospheric pressure until no more gas was absorbed. The red-brown solution was centrifuged to remove insoluble matter. Red crystals of $[\text{Ni}(\text{NO})(\eta^5\text{-Cp}^*)]$ were obtained after slow evaporation of pentane. Because $[\text{Ni}(\text{NO})(\eta^5\text{-Cp}^*)]$ is air and moisture sensitive, all manipulations were carried out under an inert atmosphere. Pentane used in the experiment was washed with concentrated H_2SO_4 , dried with MgSO_4 , and distilled.

The prismatic crystal selected for the X-ray diffraction experiment was placed in a borosilicate glass capillary, which was partially silver-coated for better heat conductivity. The capillary was attached to the cold finger of a diffractometer-mounted⁸ closed-cycle DISPLEX helium cryostat (Air Products and Chemicals Inc.). An XTRANS carbon-fiber chamber (Anholt Technologies Inc.) with a light-transparent window was used to provide both X-ray and visible light access to the crystal, while maintaining the necessary vacuum environment around the capillary.

Data Collection. X-ray intensities were collected on a Huber four-circle diffractometer using graphite-monochromated $\text{Mo K}\alpha$ radiation from a Rigaku Corp. rotating-anode ROTAFLEX generator (60 kV, 90 mA). A half-cylinder-shaped ($r = 90$ mm) imaging plate (IP) holder was mounted on the diffractometer coaxially with the φ axis. This arrangement allows reflections with 2θ values up to 110° to be measured. An "antiscatter device" was introduced into the XTRANS carbon-fiber chamber to shield the imaging plate from the scattering by the walls of the chamber.⁹ Fuji HR-IIIIN imaging plates, a Fuji BAS2000 scanner, and visualization software were employed. Data were collected with 4° φ oscillations of 4 min exposure time each, at 25 K. During the experiment, the temperature was monitored with a silicon diode thermometer (Scientific Instruments, Inc.).

Two data sets were collected on the same crystal in the ground and mixed ground/metastable states. The metastable state was generated by irradiating the crystal at 25 K for 3 h with 458 nm light from an Ar^+ laser, with a power of 150 mW/cm². As observed in our previous studies of light-induced metastable states,^{1,2} a significant change in cell dimensions occurs upon irradiation. The crystallographic b axis, along which NO is oriented, decreased from 14.355(3) to 14.078(10) Å upon increasing conversion to the metastable state, while the c axis lengthened to a lesser extent. The shortening of the b axis and changes in reflection intensities, the latter illustrated in Figure 1, were subsequently monitored to ensure maximum conversion to the metastable state before the data collection was started. Crystal data and X-ray data collection details are summarized in Table 1.

Data Reduction. The seed-skewness method based program HIPPO¹⁰ was used for peak integration. The program XEMP, which is a part of the SHELXTL PC¹¹ package, was used for the empirical absorption correction of the data. The program SORTAV¹² modified to handle IP data was used for sorting, scaling, and averaging.

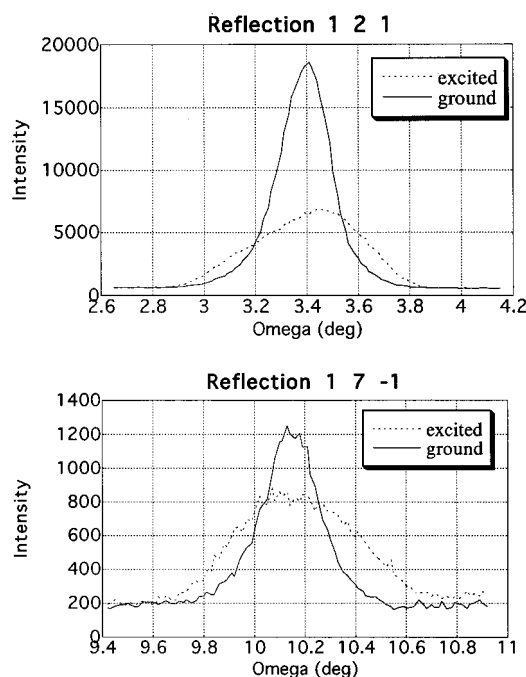


Figure 1. Change of profiles and intensities of some reflections upon excitation.

Table 1. X-ray Experimental Data for $[\text{Ni}(\text{NO})(\eta^5\text{-Cp}^*)]$

	ground state	excited/ground state
empirical formula	$\text{C}_{10}\text{H}_{15}\text{NONi}$	$\text{C}_{10}\text{H}_{15}\text{NONi}$
formula weight	223.7	223.7
space group	$P2_1/c$	$P2_1/c$
temp (K)	25	25
a (Å)	11.874(3)	11.894(5)
b (Å)	14.355(3)	14.078(10)
c (Å)	12.094(3)	12.208(7)
β (deg)	90.25(1)	90.13(1)
V (Å ³)	2061.4	2044.2
Z	8	8
d_{calc} (g/cm ³)	1.443	1.455
abs coeff (cm ⁻¹)	1.92	1.93
transm		0.389–0.476
crystal dimens (mm)		$0.375 \times 0.125 \times 0.10$
radiation wavelength (Å)	0.7107	0.7107
range of $(\sin \theta)/\lambda$ (Å ⁻¹)	0.11–0.90	0.11–0.89
h,k,l		
lower limit	–19,0,0	–18,0,0
upper limit	20,23,20	17,19,18
no. of reflns measd	32 416	23 996
no. of symm-unique reflns	3805	2205
merging factor R (%)	3.2	3.0
no. of params in the refinement	326	208
$R_1(F)$ (%)	4.1	5.0
$wR_2(F^2)$ (%)	8.0	9.8
GOF	1.12	1.14
residuals on diff Fourier map (e/Å ³)		
max	0.62	0.66
min	0.54	0.55

All least-squares refinements were done with the SHELXL93¹³ structure refinement package.

Computational Details. All theoretical calculations reported below were carried out using either Hartree–Fock or density functional theory (DFT) with the Gaussian 94 package.¹⁴ The hybrid functional B3LYP¹⁵ was employed for the DFT calculations. Complete geometry optimizations of the structures of $[\text{Ni}(\text{NO})(\eta^5\text{-Cp}^*)]$, $[\text{Ni}(\eta^2\text{-NO})(\eta^5\text{-Cp}^*)]$, and $[\text{Ni}(\text{ON})(\eta^5\text{-Cp}^*)]$ were performed using the effective core potential (ECP) basis set LANL2DZ, which was introduced by Hay and Wadt.¹⁶ The geometry optimization for the ground-state structure was carried

- (6) White, M. A.; Pressprich, M. R.; Coppens, P.; Coppens, D. D. *J. Appl. Crystallogr.* **1994**, 27, 717.
- (7) Piper, T. S.; Cotton, F. A.; Wilkinson, G. *J. Inorg. Nucl. Chem.* **1955**, 1, 165.
- (8) Henriksen, K.; Larsen, F. K.; Rasmussen, S. E. *J. Appl. Crystallogr.* **1986**, 19, 390. Graafma, H.; Sagerman, G.; Coppens, P. *J. Appl. Crystallogr.* **1991**, 24, 961.
- (9) Darovsky, A.; Bolotovskiy, R.; Coppens, P. *J. Appl. Crystallogr.* **1994**, 27, 1039.
- (10) Bolotovskiy, R.; White, M. A.; Darovsky, A.; Coppens, P. *J. Appl. Crystallogr.* **1995**, 28, 86.
- (11) Sheldrick, G. M. *SHELXTL PC User's Manual*; Siemens Analytical X-ray Instruments Inc.: Madison, WI, 1990.
- (12) Blessing, R. H. *Crystallogr. Rev.* **1987**, 1, 3.

- (13) Sheldrick, G. M. *SHELXL93: Program for the Refinement of Crystal Structures*; University of Göttingen: Göttingen, Germany, 1993.

Table 2. Selected Bond Lengths (Å) for Ground-State and Metastable-State Structures of [Ni(NO)(η^5 -Cp*)] at 25 K

bond	ground state		metastable state	
	molecule A	molecule B	molecule A	molecule B
Ni—N	1.620(3)	1.614(3)	1.697(18)	1.724(10)/1.716(10)
Ni—O			2.096(18)	2.077(10)/2.079(10)
Ni—plane ^a	1.719(1)	1.718(1)	1.732(6)	1.750(6)
Ni—C1	2.107(3)	2.110(3)	2.092(12)	2.138(12)
Ni—C2	2.106(3)	2.110(3)	2.132(12)	2.132(11)
Ni—C3	2.109(3)	2.108(3)	2.142(11)	2.137(12)
Ni—C4	2.106(3)	2.104(3)	2.142(12)	2.120(12)
Ni—C5	2.105(3)	2.110(3)	2.106(12)	2.165(12)
N—O	1.177(3)	1.181(4)	1.134(18)	1.126(30)/1.128(32)
C1—C2	1.437(4)	1.443(4)	1.456(14)	1.441(13)
C1—C5	1.434(4)	1.438(4)	1.412(13)	1.467(13)
C2—C3	1.436(5)	1.430(4)	1.454(13)	1.451(13)
C3—C4	1.433(5)	1.430(4)	1.473(14)	1.421(13)
C4—C5	1.425(4)	1.436(4)	1.434(13)	1.445(13)
C1—C6	1.501(5)	1.500(4)	1.521(13)	1.520(13)
C2—C7	1.507(4)	1.499(4)	1.504(14)	1.515(14)
C3—C8	1.506(4)	1.507(4)	1.523(13)	1.513(13)
C4—C9	1.503(5)	1.501(4)	1.512(14)	1.515(13)
C5—C10	1.503(4)	1.498(4)	1.514(13)	1.483(14)

^a The mean plane through the C1, C2, C3, C4, C5 atoms of the Cp* ring.

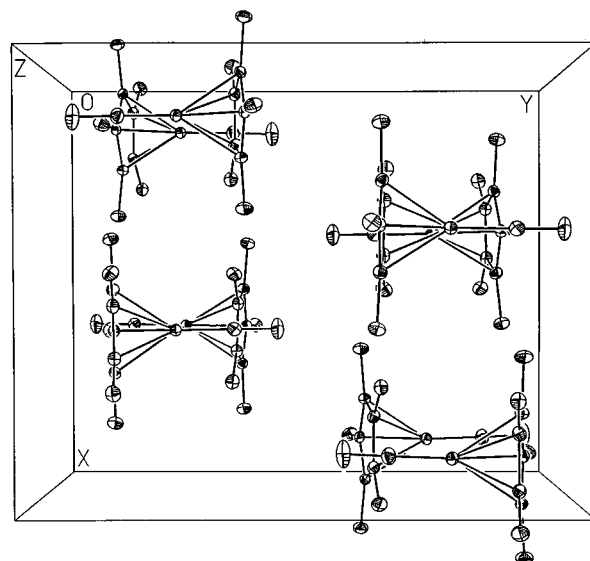
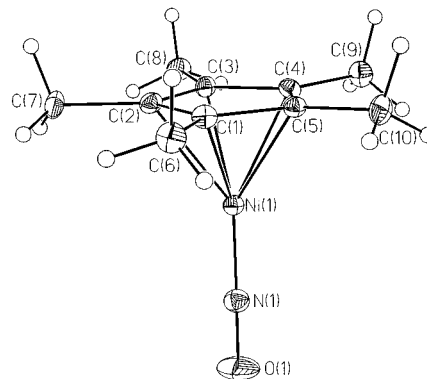
Table 3. Selected Angles (deg) for Ground-State and Metastable-State Structures of [Ni(NO)(η^5 -Cp*)] at 25 K

angle	ground state		metastable state	
	molecule A	molecule B	molecule A	molecule B
C1—C2—C3	107.9(3)	107.8(3)	118(1)	110(1)
C2—C3—C4	108.2(3)	108.5(3)	96(1)	109(1)
C3—C4—C5	108.2(3)	108.0(3)	115(1)	111(1)
C4—C5—C1	107.8(3)	107.9(3)	108(1)	103(1)
C5—C1—C2	107.9(3)	107.8(3)	103(1)	112(1)
C6—C1—C2	126.3(3)	126.6(3)	130(1)	129(1)
C7—C2—C3	125.8(3)	125.5(3)	123(1)	130(1)
C8—C3—C4	126.0(3)	124.8(3)	131(1)	131(1)
C9—C4—C5	126.4(3)	125.7(3)	126(1)	130(1)
C10—C5—C1	126.1(3)	125.8(3)	126(1)	136(1)
Ni—N—O	179.2(3)	179.1(3)	93(1)	91(1)/92(1)

out under both C_5 and C_1 symmetries. Stability tests were performed on the wave functions for each optimized geometry to ensure that they correspond to the electronic ground state. In addition, vibrational analyses were carried out for all optimized geometries to ensure that they are true stationary points on the potential energy surface. For comparative purposes, the ground-state structure was also optimized at the DFT level using a standard 3-21G and a mixed basis set denoted as 3-21G-M. The 3-21G-M basis set consisted of a 6-31G(d) basis for the N and O, a 6-311+G basis for the Ni, and 3-21G basis for the C and H atoms.

Results

The Ground-State Structure. The ground-state structure of [Ni(NO)(η^5 -Cp*)] was solved by the Patterson method. The asymmetric unit contains two independent molecules, referred to as A and B in the following discussion. Positions of all non-hydrogen atoms were obtained from the subsequent difference

**Figure 2.** Packing diagram of the crystal structure of [Ni(NO)(η^5 -Cp*)] in the ground state. Hydrogen atoms are omitted for clarity. 50% probability ellipsoids are shown.**Figure 3.** ORTEP drawing of molecule A in the ground state. 50% probability ellipsoids are shown, except for those of the H atoms.

Fourier synthesis; all non-hydrogen atoms were refined with anisotropic temperature factors. Positions of the hydrogen atoms were located from the difference Fourier map and refined isotropically with a common temperature factor. The agreement factors after full-matrix least-squares refinement are $R_1(F) = 4.1\%$ and $wR_2(F^2) = 8.0\%$. Selected bond lengths and angles are presented in Tables 2 and 3. The highest residual peak in the difference Fourier synthesis is $0.62 \text{ e}/\text{\AA}^3$, located 0.73 \AA from the position of the nickel atom of molecule B, and the deepest minimum is $-0.54 \text{ e}/\text{\AA}^3$, which is 0.74 \AA from the nickel atom of molecule A. A packing diagram of the structure and an ORTEP plot of molecule A are shown in Figures 2 and 3, respectively.

Structure of the Light-Induced Metastable State. In the first stage of the analysis, the partially excited crystal was treated as containing a single species. Starting positions for all atoms were taken from the ground-state structure, and only the scale factor was allowed to refine, giving agreement factors $R_1 = 13.5\%$ and $wR_2 = 29.5\%$. Subsequent difference Fourier synthesis showed several strong residual peaks ranging from a maximum of $4.3 \text{ e}/\text{\AA}^3$ to a minimum of $-3.7 \text{ e}/\text{\AA}^3$. A difference Fourier map which illustrates the features in the vicinity of the Ni—N—O group of molecule A is presented in Figure 4. A similar map was obtained for molecule B. These maps indicate a reorientation of the nitrosyl group atoms upon excitation, accompanied by a shift of the nickel atom.

- (14) Frisch, M. J.; Trucks, G. W.; Schlegel, H. B.; Gill, P. M. W.; Johnson, B. G.; Robb, M. A.; Cheeseman, T. A.; Keith, T. A.; Petersson, G. A.; Montgomery, J. A.; Raghavachari, K.; Al-Laham, M. A.; Zakrzewski, V. G.; Ortiz, J. V.; Foresman, J. B.; Cioslowski, B.; Stefanov, B.; Nanayakkara, A.; Challacombe, M.; Peng, C. Y.; Ayala, P. Y.; Chen, W.; Wong, M. W.; Andres, J. L.; Replogle, E. S.; Gomperts, R.; Martin, R. L.; Fox, D. J.; Binkley, J. S.; Defrees, D. J.; Baker, J.; Stewart, J. P.; Head-Gordon, M.; Gonzalez, C.; Pople, J. A. *Gaussian 94*; Gaussian Inc.: Pittsburgh, PA, 1994.
- (15) Becke, A. D. *J. Chem. Phys.* **1993**, *98*, 5648. Lee, C.; Yang, W.; Parr, R. *Phys. Rev. B* **1988**, *37*, 785.
- (16) Hay, P. J.; Wadt, W. R. *J. Chem. Phys.* **1985**, *82*, 270, 299.

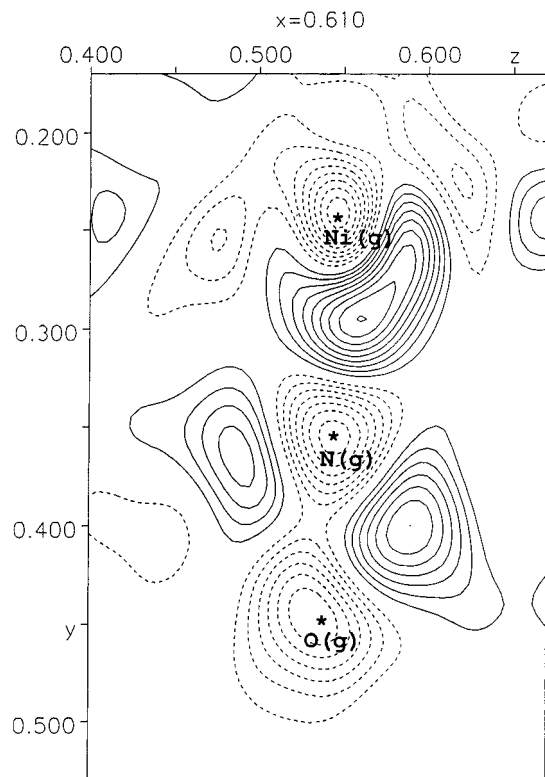


Figure 4. Difference between the electron density in the excited crystal and the ground-state density in a section containing the Ni, N, and O atoms. Contours are at $0.4 \text{ e}/\text{\AA}^3$. Negative contours are dotted; positive contours full.

Since not all molecules in the crystal are transferred into the metastable state, proper refinement of this crystal structure requires the incorporation of both ground- and metastable-state components in the scattering formalism. Our formalism, which has been successfully tested in earlier studies,^{1,2} is based on a random distribution of the two species. To obtain the structure of the metastable state, the ground-state molecule $[\text{Ni}(\text{NO})(\eta^5\text{-Cp}^*)]$ was treated as a pseudorigid body by applying restraints. Bond lengths between non-hydrogen atoms obtained in the course of the ground-state structure refinement were used as the target values for the restraints. Weights of the restraints were constructed as $1/\sigma^2$, where σ is the estimated standard deviation of the particular bond from the ground-state refinement. The initial population of the ground state was arbitrarily set to 50%. The positional parameters of the atoms of the metastable species were allowed to refine, together with the population of the metastable state. In this refinement, the temperature parameters of all atoms except Ni, N, and O were fixed at their ground-state values. The temperature parameters of Ni in the metastable state were refined anisotropically, and those of N and O isotropically. The populations of the species in the metastable state were obtained in the least-squares refinement as 47.5(9)% and 46(1)% for the A and B molecules, respectively. An ORTEP plot of molecule A in the metastable state is shown in Figure 5. The situation is more complicated for molecule B, which shows a disorder in the position of the NO group. Two possible orientations for NO occur with populations of 28(1)% and 18(1)%, respectively. ORTEP plots showing the positions of the NO group with respect to the carbon atoms of the pentamethylcyclopentadienyl ring for the A and B molecules are presented in Figure 6.

In the mixed ground/metastable-state refinement, all bond lengths between non-hydrogen atoms of the ground-state

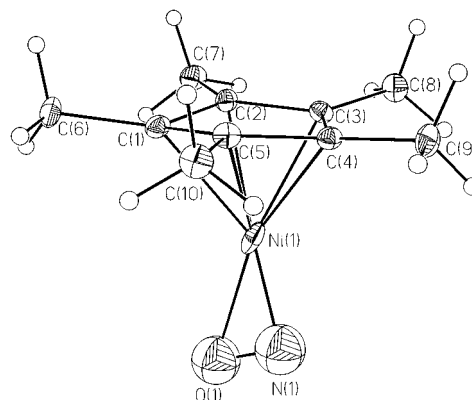


Figure 5. ORTEP drawing of molecule A in the light-induced metastable state. 50% probability ellipsoids are shown, except for those of the H atoms.

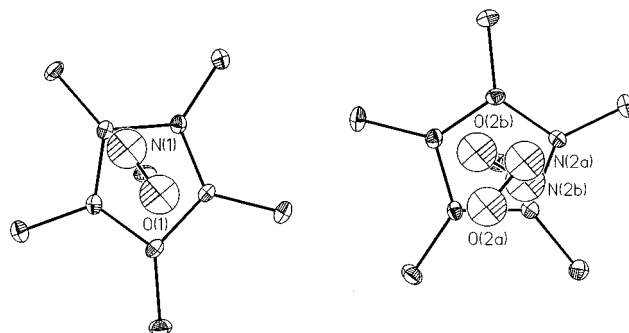


Figure 6. ORTEP drawing of the A (left) and B (right) metastable molecules in the asymmetric unit, showing two positions for the NO group for molecule B. 50% probability ellipsoids are shown. Hydrogen atoms are omitted for clarity.

molecule remained within one standard deviation of corresponding values from the refinement of the ground-state structure.

The most important geometrical change upon excitation is a decrease in the Ni–N–O angle from $179.2(2)$ and $179.1(3)$ to $93(1)$ and $91(1)^\circ$ for the A and B molecules, respectively. As a result, the Ni–O distances are reduced to values typical for a bonding interaction, as discussed further below. A lengthening of the Ni–N distances by $0.08(1)$ and $0.10(1) \text{ \AA}$ and shifts of Ni away from the Cp* rings were also observed. The distance between Ni and the mean plane through the five-membered ring increases by $0.013(6)$ and $0.032(6) \text{ \AA}$ in the A and B molecules, respectively. The average displacement of the carbon atoms of the methyl groups from the mean plane of the ring, in a direction away from the Ni atom, increases by $0.086(30)$ and $0.094(30) \text{ \AA}$ for the two molecules.

The mixed ground/metastable-state structure was refined to $R_1(F) = 5.1\%$ and $wR_2(F^2) = 9.8\%$; the largest correlation coefficient (0.92) was between the positional parameters of the nickel atoms in the ground and metastable states. The highest remaining peak in the difference Fourier synthesis was $0.66 \text{ e}/\text{\AA}^3$ at 1.1 \AA from the position of Ni of the B molecule, and the deepest minimum was $-0.55 \text{ e}/\text{\AA}^3$ at 0.96 \AA from the position of one of the carbon atoms. The bond lengths and angles of the metastable-state structure are summarized in Tables 2 and 3, respectively. The riding model was used for the refinement of hydrogen atoms in the mixed ground/metastable-state structure. In this model, the C–H vector remains constant in magnitude (0.98 \AA) and direction, but the carbon atom can move.

Computational Results. As mentioned earlier, full geometry optimizations were performed at the DFT level for the ground

Table 4. Calculated and Experimental Structural Parameters (Å), Total Energies, and Vibrational Frequencies of NO for the Ground-State Structure of [Ni(NO)(η^5 -Cp*)]^a

	HF	B3LYP			exptl ^b
	LANL2DZ	3-21G	3-21G-M	LANL2DZ	
Ni–C(ring)	2.202	2.033	2.158	2.188	2.107
Ni–N	1.584	1.592	1.616	1.628	1.620
N–O	1.167	1.210	1.174	1.214	1.177
C–C	1.432	1.445	1.442	1.448	1.433
C–C(CH ₃)	1.507	1.498	1.507	1.507	1.504
C–H	1.083	1.095	1.095	1.096	0.962
ν (NO) (cm ⁻¹)		1680	1916	1836	1786
total energy (hartrees)	–684.5840	–2018.3313	–2026.2573	–689.2808	

^a Calculations reported here were carried out under C₅ point group symmetry. ^b Average distances in molecule A.

Table 5. Calculated and Experimental Structural Parameters (Å) for the Metastable-State Structure of [Ni(NO)(η^5 -Cp*)]^a and Calculated Structural Parameters for [Ni(ON)(η^5 -Cp*)]^b

	[Ni(η^2 -NO)(η^5 -Cp*)]		[Ni(ON)(η^5 -Cp*)]
	B3LYP/LANL2DZ	exptl ^c	B3LYP/LANL2DZ
Ni–C(1)	2.117	2.092(12)	2.191
Ni–C(2)	2.200	2.132(12)	2.191
Ni–C(5)		2.106(12)	
Ni–C(3)	2.236	2.142(11)	2.191
Ni–C(4)		2.142(12)	
Ni–N	1.740	1.697(18)	–
Ni–O	2.121	2.096(18)	1.697
N–O	1.278	1.134(18)	1.224
C(1)–C(2)	1.460	1.456(14)	1.448
C(1)–C(5)		1.412(13)	
C(2)–C(3)	1.436	1.454(13)	1.448
C(4)–C(5)		1.434(13)	
C(3)–C(4)	1.455	1.473(14)	1.448
C–C(CH ₃)	1.507	1.515(14)	1.507
C–H	1.096	0.98	1.096
Ni–N–O (deg)	87.9	93(1)	180
total energy (hartrees)	–689.2443		–689.2128

^a [Ni(η^2 -NO)(η^5 -Cp*)] structure optimization was carried out under C₁ point group symmetry. ^b [Ni(ON)(η^5 -Cp*)] structure optimization was carried out under C₅ point group symmetry. ^c Distances for molecule A in the metastable state.

state, the experimentally observed metastable state, and a hypothetical isonitrosyl structure. Optimization of the ground-state structure under C₁ and C₅ symmetries yielded structures which differed by less than 0.004 eV in total energy and had negligible differences in geometry. Accordingly they are considered the same for the purpose of the present study. Table 4 shows the results of geometry optimizations carried at both the DFT and HF levels for [Ni(NO)(η^5 -Cp*)] in the ground state with various basis sets. Total energies and calculated and experimentally obtained frequencies for the stretching vibrations of NO are also listed in Table 4. Table 5 contains the results of geometry optimization for the [Ni(η^2 -NO)(η^5 -Cp*)] and [Ni(ON)(η^5 -Cp*)] structures at the DFT level using a LANL2DZ basis set. Calculated Kohn–Sham orbital energies, obtained with the B3LYP functional and LANL2DZ basis set, are given in Table 6 for all three structures.

Discussion

The Ground-State Structure. Surprisingly, the crystal structure of [Ni(NO)(η^5 -Cp*)] has been never published before. The molecular structure of the cyclopentadienyl analogue of [Ni(NO)(η^5 -Cp*)] was determined in the gas phase by analysis of the microwave spectra of isotopically substituted species¹⁷ and by electron diffraction.¹⁸ Our data are in good agreement with the former results, which are more accurate, concerning

the linear geometry of the Ni–N–O group and Ni–C, Ni–N, and C–C bond lengths. The largest difference between the two structures (0.014(7) Å in the N–O bond length) is barely significant, but could be due to larger π^* back-donation from the Ni(η^5 -Cp*) fragment, which is more electron-rich than Ni(η^5 -Cp). A similar difference occurs between the C–O distances in [Mn(CO)₃(η^5 -Cp*)]¹⁹ and [Mn(CO)₃(η^5 -Cp)],²⁰ for which the average C–O bond lengths are 1.17 and 1.13 Å respectively.

Examination of the Cambridge Structural Data Base (CSD) shows that the Cp*–Ni and Ni–N distances fall in the ranges typical for the organometallic complexes of Ni. At the same time, the N–O bond is among the longest observed for the nickel nitrosyls. This effect either may be due to large π^* back-donation from the Ni(η^5 -Cp*) or may be a result of the very low temperature of the data collection, which minimizes the apparent shortening of the bond lengths due to thermal motion, an effect that can be quite large for the room-temperature structures found in the CSD.

The DFT calculations on the ground-state structure (Table 4) show that the largest discrepancy between theory and experiment occurs for the distance between the nickel atom and the pentamethylcyclopentadienyl ring. The experimental and theoretical Ni–C distances differ by more than 0.05 Å in all cases. The LANL2DZ basis set does not reproduce the N–O bond length very well either. Much better results were obtained with the all-electron calculation employing the 3-21G-M basis set. All basis sets reproduce geometry of the Cp* fragment quite accurately; differences from the experimental values did not exceed 0.01 Å. Overall, the structure optimized with the 3-21G-M basis set shows the best agreement with experiment.

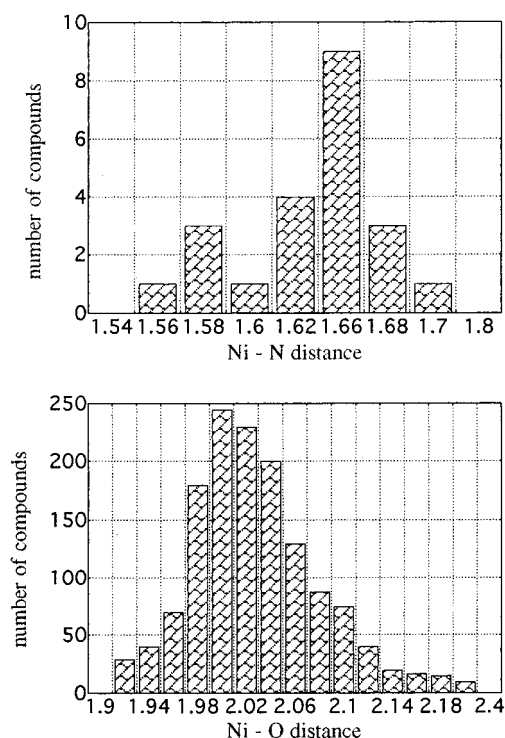
Since all calculations for the metastable-state structures were carried out under C₁ symmetry, the computationally less demanding LANL2DZ basis set was employed in the corresponding geometry optimizations. As is evident from Table 4, this basis set yields results which are in reasonable agreement with the experimental geometry for the ground state.

Structure of the Metastable State. Structures with the η^2 -bound nitrosyl have never been experimentally observed for the {M(NO)}¹⁰ family. To our knowledge, the first and only example of side-bound nitrosyl is the structure of sodium nitroprusside (SNP) in the second metastable state (MS₂).¹ There

- (17) Cox, A. P.; Brittain, A. H. *J. Chem. Soc., Faraday Trans.* **1970**, 66, 557.
- (18) Ronova, I. A.; Alekseeva, N. V.; Veniaminov, N. N.; Kravets, M. A. *J. Struct. Chem. (Engl. Transl.)* **1975**, 16, 441.
- (19) Fortier, S.; Baird, M. C.; Preston, K. F.; Morton, J. R.; Ziegler, T.; Jaeger, T. J.; Watkins, W. C.; MacNeil, J. H.; Watson, K. A.; Hensel, K.; Le Page, Y.; Charland, J. P.; Williams, A. J. *J. Am. Chem. Soc.* **1991**, 113, 542.
- (20) Fitzpatrick, P. J.; Le Page, Y.; Sedman, J.; Butler, I. S. *Inorg. Chem.* **1981**, 20, 2852.

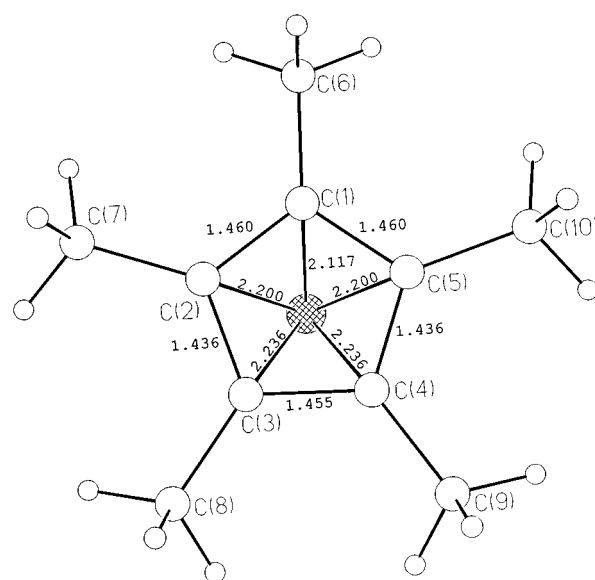
Table 6. Kohn–Sham Orbital Energies (eV) for $[\text{Ni}(\text{NO})(\eta^5\text{-Cp}^*)]$, $[\text{Ni}(\eta^2\text{-NO})(\eta^5\text{-Cp}^*)]$, and $[\text{Ni}(\text{ON})(\eta^5\text{-Cp}^*)]$ Molecules

orbital	C ₅ point group		orbital	C _s point group [$\text{Ni}(\eta^2\text{-NO})(\eta^5\text{-Cp}^*)$]
	[$\text{Ni}(\text{NO})(\eta^5\text{-Cp}^*)$]	[$\text{Ni}(\text{ON})(\eta^5\text{-Cp}^*)$]		
e ₁ (LUMO)	−2.17	−2.58	a'	−2.10
e ₁ (HOMO)	−5.53	−5.03	a''(LUMO)	−2.78
e ₂	−7.35	−6.94	a''(HOMO)	−5.27
a	−7.51	−7.09	a'	−5.65
e ₁	−7.94	−7.33	a''	−7.31
			a''	−7.49
			a'	−7.78

**Figure 7.** Frequency of occurrence of Ni–N distances for the nickel nitrosyl complexes listed in the Cambridge Structural Data Base (upper plot) and frequency of occurrence of Ni–O distances for four-coordinate nickel (lower plot).

are similarities between the metal nitrosyl geometries found in $[\text{Ni}(\eta^2\text{-NO})(\eta^5\text{-Cp}^*)]$ and SNP (MS₂) regarding elongation of the (Ni, Fe)–N bonds and the (Ni, Fe)–O distances, the latter being 2.09 and 2.07 Å for Ni and Fe, respectively. In both cases, we were not able to detect a significant elongation of the N–O bond in the metastable state, even though it would be expected from the decrease in the NO stretching frequency in the metastable state by almost 200 cm^{−1} for SNP²¹ and by 447 cm^{−1} for $[\text{Ni}(\text{NO})(\eta^5\text{-Cp})]$.⁴ Results of the DFT calculations performed by Delley²² on SNP and results of our calculations (Table 5) show a modest elongation of the N–O bond by 0.03 and 0.06 Å, respectively. Even if absolute numbers prove not to be very reliable, the trend for elongation of the N–O bond in a side-bound configuration is clear. Further studies are needed to resolve discrepancy with the crystallographic values. We note that similar discrepancies between spectroscopic and crystallographic results have been reported for related η^1 - and η^2 -acyl complexes.²³

The most important finding, which distinguishes the metastable-state structure from those of “bent nitrosyls”, is a comparatively short (2.09 Å) Ni–O distance. Histograms of Ni–N distances in nickel nitrosyls and Ni–O distances in four-coor-

**Figure 8.** Geometry of the NiCp* fragment of $[\text{Ni}(\eta^2\text{-NO})(\eta^5\text{-Cp}^*)]$ in the light-induced metastable state from optimization with the B3LYP method and the LANL2DZ basis set. N and O atoms are omitted for clarity.

dinate nickel complexes, as reported in the Cambridge Structural Data Base, are shown in Figure 7. It is clear that our experimental values fall in the usual range for covalent bonds between these atoms.

In the photoinduced linkage isomer, the Cp* ring is distorted as a result of the displacement of the metal from the symmetric position above the ring. At the same time, the Ni–Cp* distance is increased by an average of 0.022(8) Å (Table 2). These facts are consistent with the results of the DFT calculations for the metastable-state structure, which are summarized in Table 5 and illustrated in Figure 8. During the geometry optimization of the metastable molecule, the symmetry of the Cp* ring is reduced from C₅ to C_s, and the ring becomes puckered with a dihedral angle of 3.93° between the planes through the C(2), C(1), C(5) and the C(2), C(3), C(4), C(5) atoms, which are coplanar. Accordingly, there are three different groups of C–C and Ni–C bond lengths (Table 5). Even though the estimated standard deviations for the experimental C–C and Ni–C bond lengths for the metastable species are relatively large, the trend to a “diene-like” distortion is also evident. The observed increase in the average displacement of the methyl groups out of the mean plane through the ring carbon atoms, in a direction away from Ni, is a further manifestation of the effect of photoinduced isomerization on the Cp* geometry.

According to the results of the DFT calculations for $[\text{Ni}(\text{NO})(\eta^5\text{-Cp})]$,²⁴ which are in qualitative agreement with results

(21) Güida, J. A.; Aymonio, P. J.; Piro, O. E.; Castellano, E. E. *Spectrochim. Acta, Part A* **1993**, 49, 535.

(22) Delley, B.; Shefer, J.; Woike, Th. *J. Chem. Phys.*, in press.

(23) Tatsumi, K.; Nakamura, A.; Hofmann, P.; Stauffert, P.; Hoffmann, R. *J. Am. Chem. Soc.* **1985**, 107, 4440.

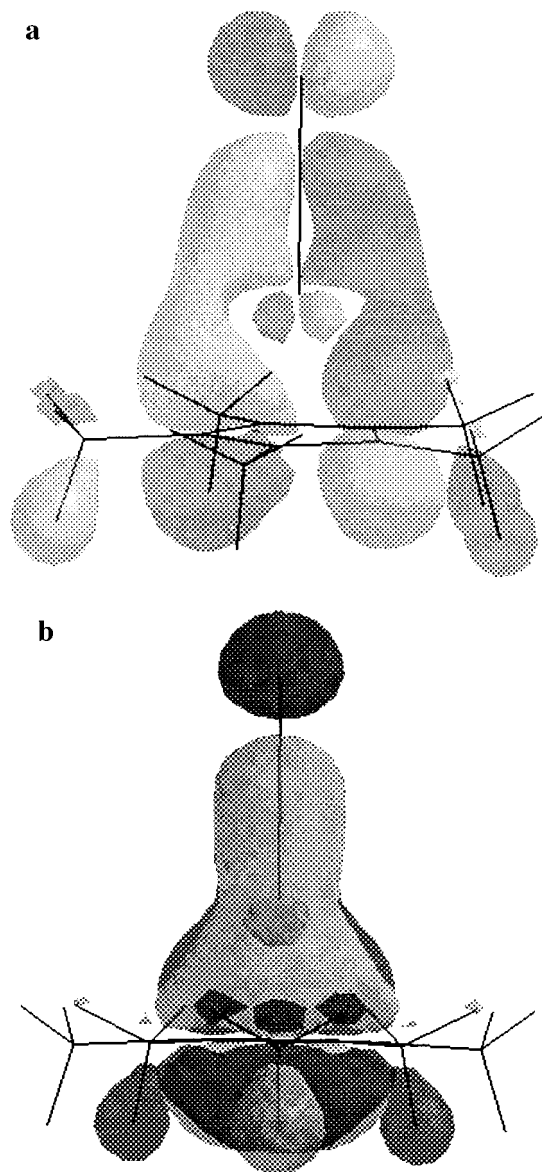


Figure 9. One member of the doubly degenerate set of the HOMO of the molecule in the ground state, shown from two different directions (a, b), calculated after geometry optimization with the B3LYP method and the LANL2DZ basis set.

of our calculations for the ground-state structure of [Ni(NO)(η^5 -Cp*)], the presence of an NO ligand with a low-lying π^* orbital of e_1 symmetry substantially stabilizes the e_1 set of orbitals of the complex, reducing the antibonding interaction between the metal d_{xz} and d_{yz} orbitals and the ring. This is illustrated in Figure 9, which shows one member of the doubly degenerate set of the HOMO of the molecule in the ground state. The overlap involving the NO, metal, and ring orbitals is evident.

As a consequence of the bending of NO, the e_1 set of orbitals of the ring is stabilized to a lesser extent than in the ground-state structure. The decrease in overlap is illustrated in Figure 10, which shows (a) the (a'') HOMO and (b) the closely spaced (a') second-highest occupied orbital of the metastable state. Compared to that of the ground state, the overlap with the e orbitals of the ring is reduced. Bonding between the metal and carbon atoms of the ring is weakened and no longer equivalent

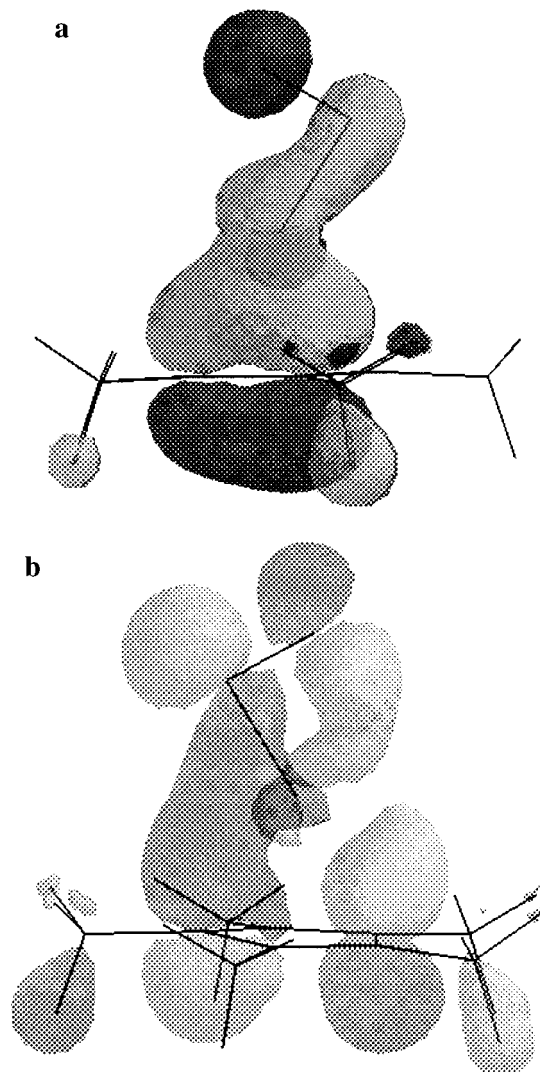


Figure 10. (a) HOMO of the light-induced metastable-state complex and (b) second-highest occupied MO for the metastable-state complex, calculated after geometry optimization with the B3LYP method and the LANL2DZ basis set. Note that illustrations a and b are different views.

for all carbon atoms. The weakening of the interaction is also evident from the crystallographically observed increase in Ni–ring distance upon photoinduced isomerization. It results in a “slip” distortion, which is well-known for [Co(CO) $_2$ (η^5 -Cp*)]²⁵ and other related compounds. We note that the second highest occupied orbital of the molecule in the metastable state (Figure 10b) shows a bonding interaction between the nickel and oxygen atoms. The observed geometry changes are in full agreement with the discussion of bonding in half-sandwich compounds given by Mingos.²⁶

The energy difference between the optimized structures of [Ni(η^2 -NO)(η^5 -Cp*)] and [Ni(NO)(η^5 -Cp*)] is 0.99 eV. This value agrees surprisingly well with the experimentally observed 1.0 eV difference between the ground state and MS₂ of SNP.²⁷

Structure of [Ni(ON)(η^5 -Cp*)]. Though the [Ni(ON)(η^5 -Cp*)] isonitrosyl structure has not been observed, our calculations show that it corresponds to a local minimum on the

(24) Field, N. C.; Green, J. C.; Mayer, M.; Nasluzov, V. A.; Rösch, N.; Siggel, M. R. F. *Inorg. Chem.* **1996**, *35*, 2504.

(25) Byers, L. R.; Dahl, L. F. *Inorg. Chem.* **1980**, *19*, 277, 680.

(26) Mingos, D. M. P. In *Comprehensive Organometallic Chemistry*; Wilkinson, G., Ed.; Pergamon: Oxford, U.K., 1985; Vol. 3, p 1.

(27) Zölner, H.; Woike, Th.; Krasser, W.; Haussühl, S. Z. *Kristallogr.* **1989**, *188*, 139.

potential energy surface. Geometrical parameters for this hypothetical molecule are also summarized in Table 5. The local minimum is about 0.86 eV higher than the energy calculated for the $[\text{Ni}(\eta^2\text{-NO})(\eta^5\text{-Cp}^*)]$ dihapto structure and 1.85 eV above that of the complex in the ground state. For SNP, the difference in energy between the two linkage isomers is only 0.1 eV.²⁷ In the latter case, both states have been observed experimentally.

Concluding Remarks

We have determined the structure of the light-induced metastable state of $[\text{Ni}(\text{NO})(\eta^5\text{-Cp}^*)]$. The side-on (η^2) bonding mode of nitric oxide, found in this complex, has never been observed for a compound with the $\{\text{M}(\text{NO})\}^{10}$ electronic configuration and differs from that of the traditional bent nitrosyl complexes, in that the Ni–O distance is reduced to a value typical for covalent bonding between these atoms.

Earlier we studied several complexes of Ru with the $\{\text{M}(\text{NO})\}^6$ configuration in which similar metastable states can be populated. Results of photochemical studies of $[\text{Mn}(\text{CO})_4(\text{NO})]$, $[\text{Mn}(\text{CO})(\text{NO})_3]$, and $[\text{Cr}(\text{NO})_4]$ conducted by Crichton and Rest^{28,29} strongly suggest that the species denoted as $[\text{Mn}(\text{CO})_4(\text{NO}^*)]$, $[\text{Mn}(\text{CO})(\text{NO})_2(\text{NO}^*)]$, and $[\text{Cr}(\text{NO})_3(\text{NO}^*)]$ similarly

are isomers with side-on (η^2) bound nitric oxide. Our studies of other transition metal nitrosyl complexes indicate that metastable linkage isomers of such complexes are quite common.³⁰

DFT methods are evidently an effective computational tool to model molecular structure not only in the ground but also in the metastable state.

Acknowledgment. Support of this work by the National Science Foundation (Grant CHE9615586) and the donors of the Petroleum Research Fund, administered by the American Chemical Society (Grant PRF28664-AC3), is gratefully acknowledged. We thank Dr. M. R. Pressprich for help in early stages of this project and Dr. M. D. Carducci for numerous discussions.

Supporting Information Available: Tables listing atomic fractional coordinates and isotropic and anisotropic thermal parameters for both ground- and metastable-state structures (6 pages). Ordering information is given on any current masthead page.

IC9713644

(28) Crichton, O.; Rest, J. A. *J. Chem. Soc., Dalton Trans.* **1978**, 202.

(29) Crichton, O.; Rest, J. A. *J. Chem. Soc., Dalton Trans.* **1978**, 208.

(30) Coppens, P.; Fomitchev, D. V.; Carducci, M. D.; Culp, K. *J. Chem. Soc., Dalton Trans.*, in press.